Results in Physics 29 (2021) 104689

Contents lists available at ScienceDirect

Results in Physics

journal homepage: www.elsevier.com/locate/rinp

Employing Hirota's bilinear form to find novel lump waves solutions to an important nonlinear model in fluid mechanics

Behzad Ghanbari

Department of Basic Science, Kermanshah University of Technology, Kermanshah, Iran

ARTICLE INFO

Keywords:
Partial differential equations
Hirota's bilinear form
Lump wave solution
Symbolic calculations

ABSTRACT

In this paper, Hirota's bilinear form has been employed to find novel lump waves solutions for the generalized Caudrey–Dodd–Gibbon–Kotera–Sawada equation. This equation is one of the most widely used equations in the field of fluid mechanics. Using the employed technique in the paper, several different categories of solutions to the equation are retrieved. Although these solutions have distinct structures, but all of them have emerged under the banner of the same method. This feature is one of the advantages of the method compared to other methods. 3D diagrams of some of the resulting solutions have also been added to the article. The techniques can be easily adopted in solving other partial differential equations.

Introduction

Many complex nonlinear models that are widely used in fluid mechanics, astronomy, biology, environment, economy, and other branches in sciences can be described via two categories of partial and ordinary differential equations [1–18]. These wide importance and applications have led to the introduction and use of different analytical and numerical methods in solving such models [19–45]. One of the most important and widely used methods in solving partial equations is the bilinear method proposed by Hirota [46]. In recent years, various improvements have been made to the method for solving partial equations or derivatives, each of which has improved the capabilities of the method. In [47], the Bogoyavlenskii–Kadomtsev–Petviashvili (BKP) equation by using Hirota's direct method and the Kadomtsev–Petviashvili (KP) hierarchy reduction method. An improved Hirota bilinear method for nonlocal complex modified Korteweg–de Vries equation is investigated in [48] where the authors showed that the equation admits multiple complex soliton solutions. The work of [49] studied lump solution and integrability for the associated Hirota bilinear equation. Then, the integrability in the sense of the Lax pair and the bilinear Bäcklund transformations was presented by the binary Bell polynomial method. A linear superposition principle of exponential traveling waves is analyzed for Hirota bilinear equations in [50] to construct a specific sub-class of N-soliton solutions formed by linear combinations of exponential traveling waves. In [51], a sufficient and necessary criterion for the existence of linear superposition principle for the exponential wave solutions to the Hirota bilinear equations were proposed. In [52], Hirota's direct method was combined with the simplified version of this method to determine the N-soliton solutions, for the Kadomtsev–Petviashvili (KP) equation. In [53], rational, interaction, and combined multi-wave solutions are obtained for Heisenberg ferromagnetic spin chain equation by using the logarithmic transformation and symbolic computation with ansatz functions. In [54], the N-dimensional Hirota bilinear equation is found, and through using the Bell polynomials, the bilinear form of the equation is derived in a very natural way. Very recently in [55], several wave solutions for the Sawada–Kotera equation and its corresponding bidirectional form are obtained using Hirota's bilinear approach.

Now, let us discuss the following generalized Caudrey–Dodd–Gibbon–Kotera–Sawada equation (gCDGKS in short) [56]

$$36\mathbf{q_t} = \left(\mathbf{q_{xxxx}} + 15\mathbf{q}\mathbf{q_{xx}} + 15\mathbf{q}^3\right)_{\mathbf{x}} - \sigma_1\left[\partial_{\mathbf{x}}^{-1}\mathbf{q}\right]_{\mathbf{yy}} - \sigma_2\left(\mathbf{q_{xxy}} + 3\mathbf{q}\mathbf{q_y} + 3\mathbf{q_x}\left[\partial_{\mathbf{x}}^{-1}\mathbf{q}\right]_{\mathbf{y}}\right), \tag{1}$$

where σ_1 and σ_2 are two real constants.

This form of equation has a generalized structure and covers some known equations. In fact, through taking some specific values for the parameters in (1), the following well-known equations are derived:

- Through taking $\sigma_1 = \sigma_2 = 5$ in Eq. (1), we derive the (2 + 1)-dimensional CDGKS equation as

$$36\mathbf{q_t} = \left(\mathbf{q_{xxxx}} + 15\mathbf{q}\mathbf{q_{xx}} + 15\mathbf{q}^3\right)_{\mathbf{x}} - 5\left[\partial_{\mathbf{x}}^{-1}\mathbf{q}\right]_{\mathbf{yy}} - 5\left(\mathbf{q_{xxy}} + 3\mathbf{q}\mathbf{q_y} + 3\mathbf{q_x}\left[\partial_{\mathbf{x}}^{-1}\mathbf{q}\right]_{\mathbf{y}}\right), \tag{2}$$

  which was first studied by Konopelchenko and Dubrovsky [57].

E-mail address: b.ghanbary@yahoo.com.

https://doi.org/10.1016/j.rinp.2021.104689
Received 29 July 2021; Received in revised form 10 August 2021; Accepted 11 August 2021
Available online 22 August 2021

- Through taking $\sigma_1 = \sigma_2 = 5, \mathbf{t} = 36\tau$ and $\mathbf{q}_y = 0$ in Eq. (1), we derive

$$\mathbf{q}_\tau = \mathbf{q}_{\mathbf{xxxxx}} + 15\mathbf{q}_\mathbf{x}\mathbf{q}_{\mathbf{xx}} + 15\mathbf{q}\mathbf{q}_{\mathbf{xxx}} + 45\mathbf{q}^2\mathbf{q}_\mathbf{x}, \tag{3}$$

which was studied in [58].

Due to the wide range of applications, a wide variety of methodologies have been applied to study this equation. In [59], the Hirota bilinear form of the equation has bee studied, then several exact interaction waves by the way of vector notations was proposed. Taking the Pfaffian technique into account and certain constraints on the real constant σ_1, the Nth-order Pfaffian solution for the equation is derived in [56]. Then, one- and two-soliton and periodic wave solutions are obtained via the Nth-order Pfaffian solutions and the Hirota–Riemann method, respectively. Some results on the Caudrey–Dodd–Gibbon–Kotera–Sawada equation, including a hierarchy of bilinear with a unified structure, the proof of nonlinear superposition formula for the CDGKS equation under certain conditions, and a higher-order CDGKS equation via a Bäcklund transformation are presented in [60]. In [61], the authors have used the pseudopotential of the equation to extract its explicit form of the inverse recursion operator. Moreover, a novel Bäcklund transformation for this equation is derived in [62] from the invariance property of the scattering problem. In [63], some wave solutions to conformable time fractional version of Caudrey–Dodd–Gibbon– Sawada–Kotera equation were obtained via the extended Kudryashov's method. Moreover, the time fractional version of the equation is studied in [64] and some new soliton solutions for the equation, including hyperbolic, trigonometric, and rational types, were determined through the application of Lie symmetry and sub-equation method. The invariance properties, optimal system, and group invariant solutions for the equation are studied in [65]. By utilizing the Lie symmetry reduction, the (1 + 1)-dimensional form of the equation was also reduced to several ordinary differential equations. This paper is arranged as follows. Firstly, Hirota's bilinear form of the gCDGKS equation is presented in "Hirota's bilinear form". Then, we have constructed several distinct forms for solutions of the main equation in "The main results". Using each of these structures, different categories of solutions are introduced for the equation. To the best of the author's knowledge, the obtained structures are important and new results regarding the studied equation. Several 3D diagrams of some of the resulting solutions have also been added to this section of the article. Finally, a summary of obtained results is presented.

Hirota's bilinear form

In [66], a new direct method for constructing multiple solutions to integral nonlinear evolutionary equations was employed by Hirota. In the light of this method, the main idea is to employ a new variable transform, so that these new variables appear in the structure of solutions related to the simpler equivalent form for the equation. Some successful applications of the method can be explored in [67–71].

To employ the method in this article, we introduce the following transformation

$$\mathbf{q}(x,y,t) = 2\Big[\ln \mathbf{g}(x,y,t)\Big]_{\mathbf{xx}} = \frac{2\left(\mathbf{g}_{xx}(x,y,t)\mathbf{g}(x,y,t) - \mathbf{g}_{\mathbf{x}}(x,y,t)^2\right)}{\mathbf{g}^2(x,y,t)}. \tag{4}$$

Then, taking the bilinear differential operator of

$$\mathbb{D}_\mathbf{x}^m \mathbb{D}_\mathbf{y}^k \mathbb{D}_\mathbf{t}^n(\mathbf{g}.\mathbf{h}) = \left(\frac{\partial}{\partial x} - \frac{\partial}{\partial x'}\right)^m \left(\frac{\partial}{\partial y} - \frac{\partial}{\partial y'}\right)^k \left(\frac{\partial}{\partial t} - \frac{\partial}{\partial t'}\right)^n \times \mathbf{g}(x,y,t)\mathbf{h}(x',y',t')\Big|_{x=x',y=y',t=t'}, \tag{5}$$

into account in (1) yields the following Hirota's bilinear structure

$$\left[36\mathbb{D}_\mathbf{x}\mathbb{D}_\mathbf{t} + \mathbb{D}_\mathbf{x}^6 - \sigma_1\mathbb{D}_\mathbf{y}^2 - \sigma_2\mathbb{D}_\mathbf{x}^3\mathbb{D}_\mathbf{y}\right]\mathbf{g}\cdot\mathbf{g} = 0. \tag{6}$$

If the resulting operator in (1) is expanded, we derive the following differential form

$$\begin{aligned}&-2\sigma_1\left(\frac{\partial^2\mathbf{g}}{\partial y^2}\right)\mathbf{g} - 2\sigma_2\left(\frac{\partial^4\mathbf{g}}{\partial y\partial x^3}\right)\mathbf{g} + 6\sigma_2\left(\frac{\partial^3\mathbf{g}}{\partial y\partial x^2}\right)\frac{\partial\mathbf{g}}{\partial x} - 6\sigma_2\left(\frac{\partial^2\mathbf{g}}{\partial y\partial x}\right)\frac{\partial^2\mathbf{g}}{\partial x^2}\\&+2\sigma_2\left(\frac{\partial\mathbf{g}}{\partial y}\right)\frac{\partial^3\mathbf{g}}{\partial x^3} + 2\sigma_1\left(\frac{\partial\mathbf{g}}{\partial y}\right)^2 + 72\left(\frac{\partial^2\mathbf{g}}{\partial x\partial t}\right)\mathbf{g}\\&+2\left(\frac{\partial^6\mathbf{g}}{\partial x^6}\right)\mathbf{g} - 72\left(\frac{\partial\mathbf{g}}{\partial t}\right)\frac{\partial\mathbf{g}}{\partial x} - 12\left(\frac{\partial^5\mathbf{g}}{\partial x^5}\right)\frac{\partial\mathbf{g}}{\partial x} + 30\left(\frac{\partial^4\mathbf{g}}{\partial x^4}\right)\frac{\partial^2\mathbf{g}}{\partial x^2} - 20\left(\frac{\partial^3\mathbf{g}}{\partial x^3}\right)^2 = 0.\end{aligned} \tag{7}$$

The structure obtained in Eq. (7) is one of the most important results that is used in the subsequent parts of this paper.

The main results

In this section, different symbolic structures (mainly taken from [53]) are employed to construct the analytical solution of the equation. The main purpose of this work is to find new and different forms for the equation using the technique.

Collision of lump wave and a strip soliton

In this part, we examine the following symbolic structure

$$\mathbf{g}(x,y,t) = \eta_0 + \eta_1\tau_1^2 + \eta_2\tau_2^2 + \eta_3\exp(\tau_3), \tag{8}$$

where

$$\tau_1 = a_0 + a_1x + a_2y + a_3t, \tau_2 = b_0 + b_1x + b_2y + b_3t,$$
$$\tau_3 = c_0 + c_1x + c_2y + c_3t,$$

with a_i, b_i, c_i's are parameters need to be determined. These definitions for τ_1, τ_2, and τ_3 remain valid throughout the article.

We substitute (8) into (7) and then collect the coefficients of the same powers of similar components. Zeroing these coefficients yields a nonlinear system of equations. Due to the complexity of such resulting systems, it is usually necessary to use symbolic computing software such as Mathematica or Maple. After following the outlined steps, several categories of analytical solutions for the equation are extracted as follows:

Case 1: We derive the following values

$$\begin{aligned}&c_3 = \frac{-c_1^6 + \sigma_2c_1^3c_2 + \sigma_1c_2^2}{36c_1}, \eta_1 = 0,\\&\eta_2 = 0 \quad \& \quad c_0, c_1, c_2, \eta_0, \eta_3 = \text{free parameters}.\end{aligned} \tag{9}$$

Taking these values into account along with (8), we get

$$\mathbf{g}(x,y,t) = \eta_0 + \eta_3\exp\left(\frac{t\left(-c_1^6 + \sigma_2c_1^3c_2 + \sigma_1c_2^2\right)}{36c_1} + xc_1 + yc_2 + c_0\right). \tag{10}$$

Then using (10) and (4), we obtain the solution of (1). Numerical behaviors corresponding to Eq. (10) is presented in Fig. 1 when one takes and $\sigma_1 = 0.7, \sigma_2 = 2.5, \eta_0 = 0.6, \eta_3 = 0.8, c_0 = 0.3, c_1 = 0.01, c_2 = 1, c_3 = 0.3$ are taken.

Case 2: We derive the following values

$$\begin{aligned}&a_3 = \frac{\sigma_1\left(a_1a_2^2\eta_1 - a_1b_2^2\eta_2 + 2a_2b_1b_2\eta_2\right)}{36\eta_1a_1^2 + \eta_2b_1^2}, b_3 = \frac{\sigma_1\left(2a_1a_2b_2\eta_1 - a_2^2b_1\eta_1 + b_1b_2^2\eta_2\right)}{36\eta_1a_1^2 + \eta_2b_1^2},\\&\eta_0 = -\frac{3\sigma_2\left(a_1^5a_2\eta_1^3 + a_1^4b_1b_2\eta_1^2\eta_2 + 2a_1^3a_2b_1^2\eta_1^2\eta_2 + 2a_1^2b_1^3b_2\eta_1\eta_2^2 + a_1a_2b_1^4\eta_1\eta_2^2 + b_1^5b_2\eta_2^3\right)}{\sigma_1\eta_1\eta_2\left(a_1b_2 - a_2b_1^2\right)},\\&\eta_3 = 0 \quad \& \quad a_0, a_1, a_2, b_0, b_1, b_2, \eta_1, \eta_2 = \text{free parameters}.\end{aligned} \tag{11}$$

Taking these values into account along with (8), we get

$$\begin{aligned}\mathbf{g}(x,y,t) = &-\frac{3\sigma_2\left(\eta_1a_1^2 + \eta_2b_1^2\right)^2\left(a_1a_2\eta_1 + \eta_2b_2b_1\right)}{\sigma_1\eta_1\eta_2\left(a_1b_2 - a_2b_1\right)^2}\\&+\eta_1\left(\frac{t\sigma_1\left(a_1a_2^2\eta_1 - a_1b_2^2\eta_2 + 2a_2b_1b_2\eta_2\right)}{36\eta_1a_1^2 + \eta_2b_1^2} + xa_1 + ya_2 + a_0\right)^2\\&+\eta_2\left(\frac{t\sigma_1\left(2a_1a_2b_2\eta_1 - a_2^2b_1\eta_1 + b_1b_2^2\eta_2\right)}{36\eta_1a_1^2 + \eta_2b_1^2} + xb_1 + yb_2 + b_0\right)^2.\end{aligned} \tag{12}$$

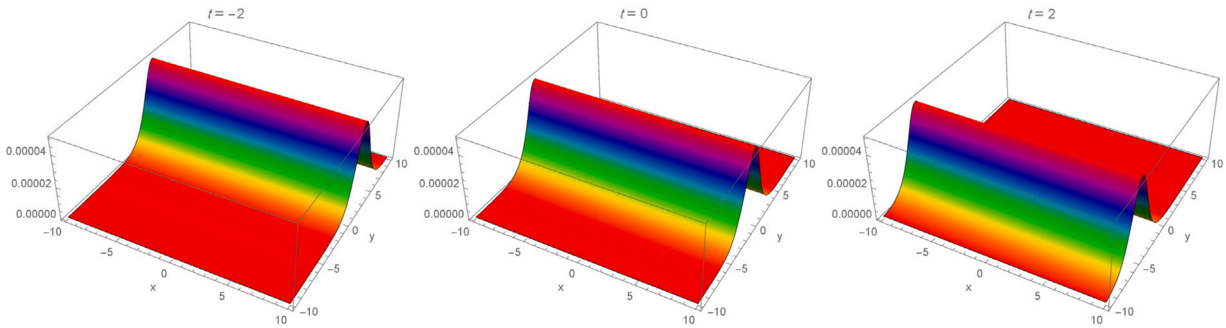

Fig. 1. Numerical simulations corresponding to Eq. (10).

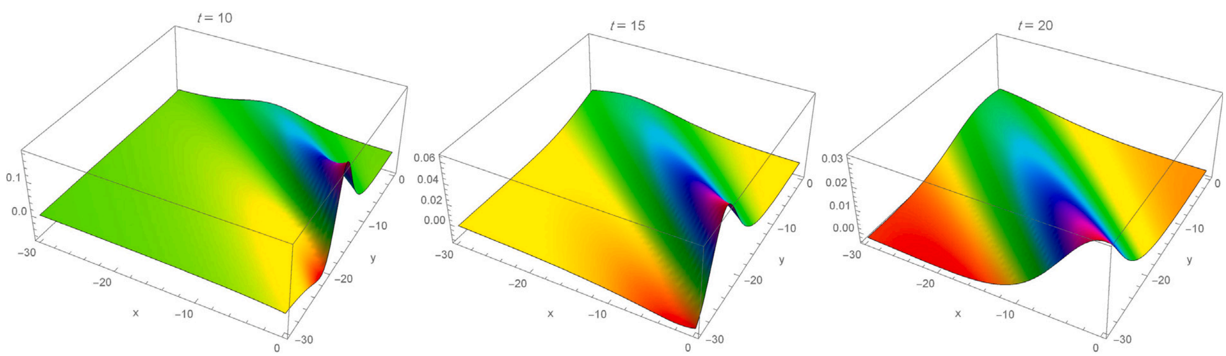

Fig. 2. Numerical simulations corresponding to Eq. (12).

Then using (12) and (4), we obtain the solution of (1). Numerical behaviors corresponding to Eq. (12) is presented in Fig. 2 when we take and $\sigma_1 = 3, \sigma_2 = 0.9, \eta_1 = 0.1, \eta_2 = 0.3, a_0 = 0.2, a_1 = 0.2, a_2 = 0.6, b_0 = 0.4, b_1 = 0.7, b_2 = 0.7$ are taken.

Case 3: We derive the following values

$$a_2 = \frac{a_1 b_2}{b_1}, a_3 =, \frac{a_1\sigma_1 b_2^2}{36b_1^2}, b_3 = \frac{\sigma_1 b_2^2}{36b_1}, \eta_2 = -\frac{\eta_1 a_1^2}{b_1^2},$$
$$\eta_3 = 0 \quad \& \quad a_0, a_1, b_0, b_1, b_2, \eta_0, \eta_1 = \text{free parameters}. \tag{13}$$

Taking these values into account along with (8), we get

$$\begin{aligned}\mathbf{g}(x,y,t) &= \eta_0 + \eta_1\left(\frac{ta_1\sigma_1 b_2^2}{36b_1^2} + xa_1 + \frac{ya_1 b_2}{b_1} + a_0\right)^2 \\ &\quad -\frac{\eta_1 a_1^2}{{b_1}^2}\left(\frac{t\sigma_1 b_2^2}{36b_1} + xb_1 + yb_2 + b_0\right)^2.\end{aligned} \tag{14}$$

Then using (14) and (4), we obtain the solution of (1).

Case 4: We derive the following values

$$a_2 = \frac{a_1 b_2}{b_1}, a_3 = \frac{a_1\left(\sigma_1 b_2^2 - 18b_1 b_3\right)}{18b_1^2}, \eta_0 = 0, \eta_2 = -\frac{\eta_1 a_1^2}{b_1^2},$$
$$\eta_3 = 0 \quad \& \quad a_0, a_1, b_0, b_1, b_2, b_3, \eta_1 = \text{free parameters}. \tag{15}$$

Taking these values into account along with (8), we get

$$\begin{aligned}\mathbf{g}(x,y,t) &= \eta_1\left(\frac{ta_1\left(\sigma_1 {b_2}^2 - 18b_1 b_3\right)}{18b_1^2} + xa_1 + \frac{ya_1 b_2}{b_1} + a_0\right)^2 \\ &\quad -\frac{\eta_1 a_1^2\left(tb_3 + xb_1 + yb_2 + b_0\right)^2}{b_1^2}.\end{aligned} \tag{16}$$

Then using (16) and (4), we obtain the solution of (1).

Numerical behaviors corresponding to Eq. (16) is presented in Fig. 3 when we take and $\sigma_1 = 2.5, \sigma_2 = 1.9, \eta_1 = 2.1, a_0 = 0.5, a_1 = 0.9, b_0 = 0.4, b_1 = 0.3, b_2 = 0.8, b_3 = 0.7$ have been taken.

Case 5: We derive the following values

$$\begin{aligned}&a_2 = \frac{5a_1 c_1^2\left(\sigma_2^2 + 4\sigma_1\right)}{12\sigma_1\sigma_2}, a_3 = \frac{25a_1 c_1^4\left({\sigma_2}^4 + 8\sigma_1\sigma^2 +_2 16{\sigma_1}^2\right)}{5184\sigma_1\sigma_2^2}, b_2 = \frac{5b_1 c_1^2\left(\sigma_2^2 + 4\sigma_1\right)}{12\sigma_1\sigma_2}, \\ &b_3 = \frac{25b_1 c_1^4\left({\sigma_2}^4 + 8\sigma_1\sigma_2^2 + 16{\sigma_1}^2\right)}{5184\sigma_1\sigma_2^2}, \\ &c_2 = -\frac{c_1^3\left(\sigma_2^2 - 20\sigma_1\right)}{12\sigma_1\sigma_2}, c_3 = -\frac{c_1^5\left(11{\sigma_2}^4 - 56\sigma_1\sigma_2^2 - 400{\sigma_1}^2\right)}{5184\sigma_1\sigma_2^2}, \eta_0 = \eta_0, \eta_1 = -\frac{\eta_2 b_1^2}{a_1^2}, \\ &a_0, a_1, b_0, b_1, c_0, c_1, \eta_2, \eta_3 = \text{free parameters}.\end{aligned} \tag{17}$$

Taking these values into account along with (8), we get

$$\begin{aligned}\mathbf{g}(x,y,t) &= \eta_0 - \frac{\eta_2 b_1^2}{a_1^2}\left(\frac{25ta_1 c_1^4\left({\sigma_2}^4 + 8\sigma_1\sigma_2^2 + 16\sigma_1^2\right)}{5184\sigma_1{\sigma_2}^2} + xa_1 + \frac{5ya_1 c_1^2\left(\sigma_2^2 + 4\sigma_1\right)}{12\sigma_1\sigma_2} + a_0\right)^2 \\ &+\eta_2\left(\frac{25tb_1 c_1^4\left({\sigma_2}^4 + 8\sigma_1\sigma_2^2 + 16{\sigma_1}^2\right)}{5184\sigma_1\sigma_2^2} + xb_1\right. \\ &\left.+\frac{5yb_1 c_1^2\left({\sigma_2}^2 + 4\sigma_1\right)}{12\sigma_1\sigma_2} + b_0\right)^2 + \eta_3 e^{-\frac{tc_1^5\left(11{\sigma_2}^4 - 56\sigma_1\sigma_2^2 - 400{\sigma_1}^2\right)}{5184\sigma_1\sigma_2^2} + xc_1 - \frac{yc_1^3\left(\sigma^2{}_2 - 20\sigma_1\right)}{12\sigma_1\sigma_2} + c_0}.\end{aligned} \tag{18}$$

Then using (18) and (4), we obtain the solution of (1). Numerical behaviors corresponding to Eq. (18) is presented in Fig. 4 when we take and $\sigma_1 = 0.7, \sigma_2 = 0.2, \eta_0 = 1.2, \eta_1 = 0.8, \eta_2 = -3, \eta_3 = -0.4, a_0 = 0.8, a_1 = 2.2, b_0 = 0.5, b_1 = 3.9, c_0 = 0.6, c_1 = 1.1$ are taken.

Collision of lump wave and a double stripes soliton

Here, the following general form is used to construct the solutions of the equation

$$\mathbf{g}(x,y,t) = \eta_0 + \eta_1\tau_1^2 + \eta_2\tau_2^2 + \eta_3\cosh(\tau_3). \tag{19}$$

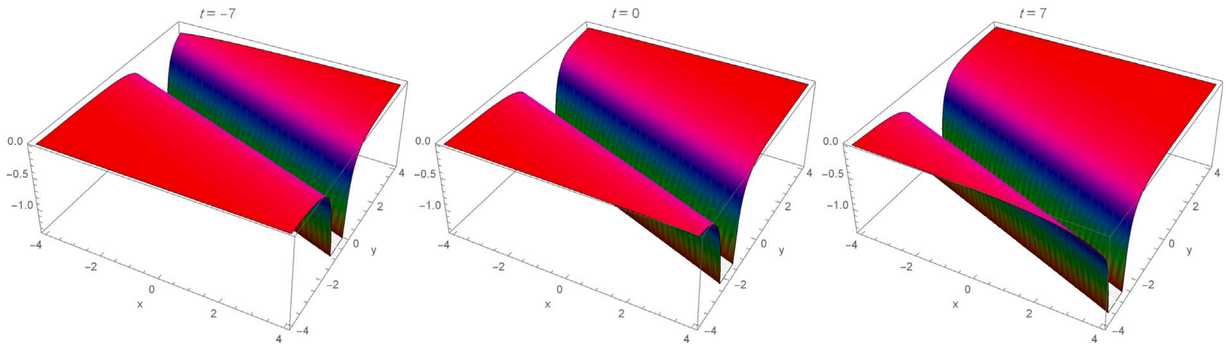

Fig. 3. Numerical simulations corresponding to Eq. (16).

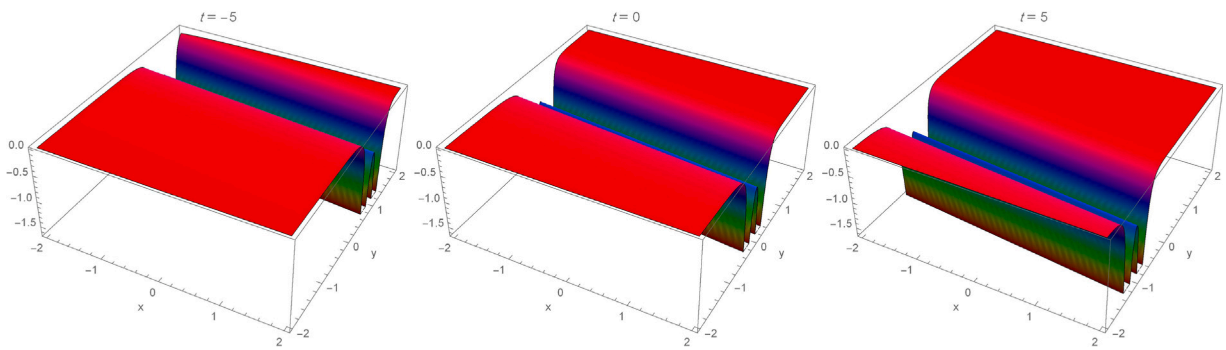

Fig. 4. Numerical simulations corresponding to Eq. (18).

Considering this structure, the following cases for the solution are introduced:

Case 1: We derive the following values

$$\begin{aligned} &c_3=\frac{-16\,c_1^6+4\,\sigma_2\,c_1^3c_2+\sigma_1\,c_2^2}{36c_1},\eta_0=0,\eta_1=0,\\ &\eta_2=0 \quad \& \quad c_0,c_1,c_2,\eta_3=\text{free parameters}. \end{aligned} \tag{20}$$

Taking these values into account along with (19), we get

$$\mathbf{g}(x,y,t)=\eta_3\cosh\left(\frac{t\left(-16\,c_1^6+4\,\sigma_2\,c_1^3c_2+\sigma_1\,c_2^2\right)}{36c_1}+xc_1+yc_2+c_0\right). \tag{21}$$

Then using (21) and (4), we obtain the solution of (1). Numerical behaviors corresponding to Eq. (21) is presented in Fig. 5 when we take and $\sigma_1=5,\sigma_2=2.5,\eta_3=5.9,c_0=0.3,c_1=0.05,c_2=1$ are taken.

Case 2: We derive the following values

$$\begin{aligned} &c_2=\frac{5c_1^3}{\sigma_2},c_3=\frac{c_1^5\left(4\,\sigma_2^2+25\,\sigma_1\right)}{36\sigma_2^2},\eta_0=\eta_0,\eta_1=0,\eta_2=0,\\ &\eta_3=\eta_3 \quad \& \quad c_0,c_1,\eta_3=\text{free parameters}. \end{aligned} \tag{22}$$

Taking these values into account along with (19), we get

$$\mathbf{g}(x,y,t)=\eta_0+\eta_3\cosh\left(\frac{tc_1^5\left(4\,\sigma_2^2+25\,\sigma_1\right)}{36\sigma_2^2}+xc_1+\frac{5yc_1^3}{\sigma_2}+c_0\right). \tag{23}$$

Lastly, utilizing (23) and (4) yields the solution of (1).

Case 3: We derive the following values

$$\begin{aligned} &c_2=\frac{5c_1^3}{\sigma_2},c_3=\frac{c_1^5\left(4\,\sigma_2^2+25\,\sigma_1\right)}{36\sigma_2^2},\eta_0=\eta_0,\eta_1=0,\\ &\eta_2=0 \quad \& \quad c_0,c_1,\eta_3=\text{free parameters}. \end{aligned} \tag{24}$$

Taking these values into account along with (19), we get

$$\mathbf{g}(x,y,t)=\eta_0+\eta_3\cosh\left(\frac{tc_1^5\left(4\,\sigma_2^2+25\,\sigma_1\right)}{36\sigma_2^2}+xc_1+\frac{5yc_1^3}{\sigma_2}+c_0\right). \tag{25}$$

Finally, from (25) and (4) the solution of (1) is introduced.

Case 4: We derive the following values

$$\begin{aligned} &a_2=-\frac{a_1c_1^2\left(\sigma_2{}^3-\sigma_2^2\sqrt{\sigma_2^2+40\,\sigma_1}+40\,\sigma_1\,\sigma_2-10\sqrt{\sigma_2^2+40\,\sigma_1}\sigma_1\right)}{2\sigma_2\sqrt{\sigma_2^2+40\,\sigma_1}\sigma_1},\\ &a_3=-\frac{a_1c_1^4\left(\sigma_2{}^5-\sigma_2{}^4\sqrt{\sigma_2^2+40\,\sigma_1}+50\,\sigma_2{}^3\sigma_1-30\,\sigma_2^2\sqrt{\sigma_2^2+40\,\sigma_1}\sigma_1+400\,\sigma_2\,\sigma_1{}^2-50\sqrt{\sigma_2^2+40\,\sigma_1}\sigma_1{}^2\right)}{72\,\sigma_2^2\sqrt{\sigma_2^2+40\,\sigma_1}\sigma_1},\\ &b_2=\frac{\left(\sigma_2^2-\sigma_2\sqrt{\sigma_2^2+40\,\sigma_1}+10\,\sigma_1\right)c_1^2b_1}{2\sigma_1\,\sigma_2},\\ &b_3=\frac{c_1^4b_1\left(\sigma_2{}^4-\sigma_2{}^3\sqrt{\sigma_2^2+40\,\sigma_1}+30\,\sigma_1\,\sigma_2^2-10\,\sigma_2\sqrt{\sigma_2^2+40\,\sigma_1}\sigma_1+50\,\sigma_1{}^2\right)}{72\,\sigma_1\,\sigma_2^2},\\ &c_2=\frac{5c_1^3}{\sigma_2},c_3=\frac{c_1^5(4\,\sigma_2^2+25\,\sigma_1)}{36\sigma_2^2},\eta_0=0,\\ &\eta_1=-\frac{\eta_2b_1^2}{a_1^2}, \quad \& \quad a_0,a_1,b_0,b_1,c_0,c_1,\eta_2,\eta_3=\text{free parameters}. \end{aligned} \tag{26}$$

Taking these values into account along with (19), we get

$$\begin{aligned} \mathbf{g}(x,y,t)=&-\frac{625\,\eta_2b_1^2}{1296\,\sigma_2{}^4\sigma_1{}^2\left(\sigma_2^2+40\,\sigma_1\right)a_1^2}\left(\left(\frac{1}{50}\,tc_1^4\sigma_2{}^4a_1+\frac{18\,c_1^2y\sigma_2{}^3a_1}{25}\right.\right.\\ &\left.+\frac{3}{5}\,\sigma_1\left(\left(tc_1^4+\frac{12\,x}{5}\right)a_1+\frac{12\,a_0}{5}\right)\sigma_2^2+\frac{36\,c_1^2y\sigma_1\,\sigma_2\,a_1}{5}+tc_1^4\sigma_1{}^2a_1\right)\\ &\left.\sqrt{\sigma^2{}_2+40\,\sigma_1}-8\left(\frac{1}{10}\,tc_1^2\sigma_2^2+tc_1^2\sigma_1+\frac{18\,y\sigma_2}{5}\right)\left(\frac{1}{40}\,\sigma_2^2+\sigma_1\right)a_1\sigma_2\,c_1^2\right)^2\\ &+\frac{25\,\eta_2}{1296\,\sigma_2{}^4\sigma_1{}^2}\left(\sigma_2\,b_1c_1^2\left(\frac{1}{10}\,tc_1^2\sigma_2^2+tc_1^2\sigma_1+\frac{18\,y\sigma_2}{5}\right)\sqrt{\sigma_2^2+40\,\sigma_1}\right.\\ &-\frac{1}{10}\,\sigma_2{}^4tb_1c_1^4-\frac{18\,\sigma_2{}^3yb_1c_1^2}{5}-3\left(\left(tc_1^4+\frac{12\,x}{5}\right)b_1+\frac{12\,b_0}{5}\right)\sigma_1\,\sigma_2^2\\ &\left.-36\,\sigma_2\,\sigma_1\,yb_1c_1^2-5\,\sigma_1^2tb_1c_1^4\right)^2\\ &+\eta_3\cosh\left(\frac{\left(4\,tc_1^5+36\,xc_1+36\,c_0\right)\sigma^2{}_2+180\,\sigma_2\,yc_1^3+25\,\sigma_1\,tc_1^5}{36\sigma_2^2}\right). \end{aligned} \tag{27}$$

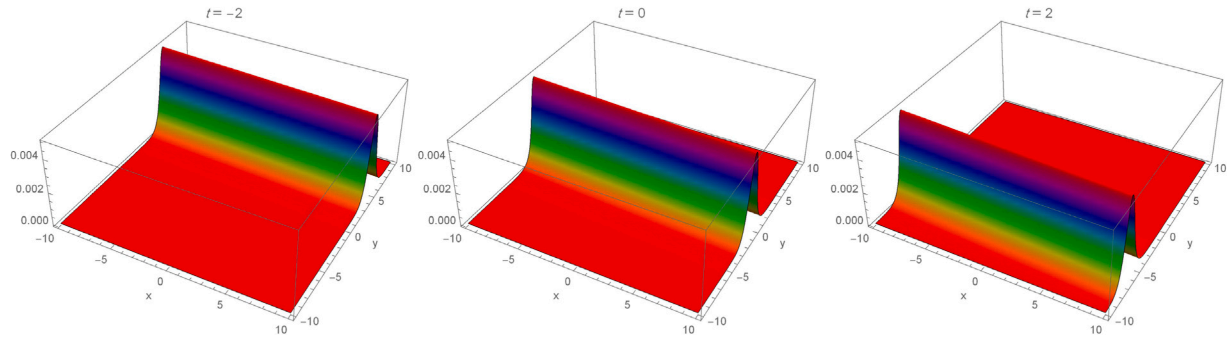

Fig. 5. Numerical simulations corresponding to Eq. (21).

Taking (27) and (4) into account, we obtain the solution of (1) is obtained.

Collision of lump and periodic waves

In this subsection, we examine the following structure for the solution of the equation

$$\mathbf{g}(x,y,t)=\eta_0+\eta_1\tau_1^2+\eta_2\tau_2^2+\eta_3\cos(\tau_3). \tag{28}$$

Taking this structure into account we find the following case for the solution:

Case 1: We derive the following values

$$\begin{aligned}
a_2&=-\frac{a_1c_1^2\left(\sigma_2{}^3+\sigma_2^2\sqrt{\sigma_2^2+40\sigma_1}+40\sigma_1\sigma_2+10\sqrt{\sigma_2^2+40\sigma_1}\sigma_1\right)}{2\sigma_2\sqrt{\sigma_2^2+40\sigma_1}\sigma_1},\\
a_3&=\frac{a_1c_1^4\left(\sigma_2{}^5+\sigma_2{}^4\sqrt{\sigma_2^2+40\sigma_1}+50\sigma_2{}^3\sigma_1+30\sigma_2^2\sqrt{\sigma_2^2+40\sigma_1}\sigma_1+400\sigma_2\sigma_1{}^2+50\sqrt{\sigma_2^2+40\sigma_1}\sigma_1{}^2\right)}{72\sigma_2^2\sqrt{\sigma_2^2+40\sigma_1}\sigma_1},\\
b_2&=-\frac{\left(\sigma_2^2+\sigma_2\sqrt{\sigma_2^2+40\sigma_1}+10\sigma_1\right)c_1^2b_1}{2\sigma_1\sigma_2},\\
b_3&=\frac{c_1^4b_1\left(\sigma_2{}^4+\sigma_2{}^3\sqrt{\sigma_2^2+40\sigma_1}+30\sigma_1\sigma_2^2+10\sigma_2\sqrt{\sigma_2^2+40\sigma_1}\sigma_1+50\sigma_1{}^2\right)}{72\sigma_1\sigma_2^2},\\
c_2&=-\frac{5c_1^3}{\sigma_2},c_3=\frac{c_1^5\left(4\sigma_2^2+25\sigma_1\right)}{36\sigma_2^2},\eta_0=\eta_0,\\
\eta_1&=-\frac{\eta_2b_1^2}{a_1^2}\quad\&\quad a_0,a_1,b_0,b_1,c_0,c_1,\eta_2,\eta_3=\text{free parameters}.
\end{aligned}\tag{29}$$

Taking these values into account along with (28), we get

$$\begin{aligned}
\mathbf{g}(x,y,t)&=\eta_0-\frac{2500\eta_2b_1^2}{81\sigma_2{}^8a_1^2\sigma_1{}^2\left(\sigma_2^2+40\sigma_1\right)}\Bigg[\Bigg(\frac{tc_1^4\sigma_2{}^4a_1}{400}-\frac{9c_1^2y\sigma_2{}^3a_1}{100}+\frac{3\sigma_1\sigma_2^2}{40}\\
&\times\left(ta_1c_1^4+\frac{12xa_1}{5}+\frac{12a_0}{5}\right)-\frac{9c_1^2y\sigma_1\sigma_2a_1}{10}+\frac{1}{8}\sigma_1{}^2ta_1c_1^4\Bigg)\\
&\sqrt{\sigma_2^6+40\sigma_1\sigma^4{}_2}+\sigma_2^3a_1\left(\frac{1}{40}\sigma_2^2+\sigma_1\right)c_1^2\left(1/10tc_1^2\sigma_2^2+tc_1^2\sigma_1-\frac{18y\sigma_2}{5}\right)\Bigg]^2\\
&+\eta_2\Bigg(-\frac{tc_1^4b_1}{36\sigma_2^2}\Bigg(-\frac{\sigma_2\left(\sigma_2{}^3+10\sigma_1\sigma_2+\sqrt{\sigma_2{}^6+40\sigma_1\sigma_2{}^4}\right)}{2\sigma_1}\\
&-\frac{5\sigma_2{}^3+50\sigma_1\sigma_2+5\sqrt{\sigma_2{}^6+40\sigma_1\sigma_2{}^4}}{\sigma_2}-5\sigma_2^2+25\sigma_1\Bigg)+xb_1\\
&-\frac{y\left(\sigma_2{}^3+10\sigma_1\sigma_2+\sqrt{\sigma_2{}^6+40\sigma_1\sigma_2{}^4}\right)c_1^2b_1}{2\sigma_1\sigma_2^2}+b_0\Bigg)^2\\
&+\eta_3\cos\left(\frac{tc_1^5\left(4\sigma_2^2+25\sigma_1\right)}{36\sigma_2^2}+xc_1-\frac{5yc_1^3}{\sigma_2}+c_0\right).
\end{aligned}\tag{30}$$

Using (30) and (4), the solution of (1) is obtained. Numerical behaviors corresponding to Eq. (30) is presented in Fig. 6 when we take and $\sigma_1=3.5,\sigma_2=3.5,\eta_0=\eta_2=0,\eta_3=10,c_0=0.9,c_1=1.7$ are taken.

Collision of lump wave and a double stripes soliton

Finally, we consider the following general structure

$$\mathbf{g}(x,y,t)=\eta_0+\eta_1\tau_1^2+\eta_2\cosh(\tau_2)+\eta_3\cos(\tau_3). \tag{31}$$

Taking this structure into account, the following case for the solution is introduced:

Case 1: We derive the following values

$$\begin{aligned}
b_2&=-\frac{b_1\left(\sigma_2^2c_1^2+\sigma_2\sqrt{\sigma_2^2+40\,\sigma_1}c_1^2-10\,\sigma_1\,b_1^2+10\,\sigma_1\,c_1^2\right)}{2\sigma_2\,\sigma_1},\\
b_3&=-\frac{5\,b_1}{36\,\sigma_1\,\sigma_2^2}\Bigg(\Bigg(\left(-\frac{1}{10}\,\sigma_2{}^3\sqrt{\sigma_2^2+40\,\sigma_1}-\frac{1}{10}\,\sigma_2{}^4\right.\\
&\left.-\sigma_2\sqrt{\sigma_2^2+40\,\sigma_1}\sigma_1-3\,\sigma_1\,\sigma_2^2-5\,\sigma_1{}^2\right)c_1^4+\left(\frac{2}{5}\,\sigma_2^2+\sigma_1\right)\\
&b_1^2\left(\sqrt{\sigma_2^2+40\,\sigma_1}\sigma_2+\sigma_2^2+10\,\sigma_1\right)c_1^2-5\,b_1^4\sigma_1\left(\frac{4\,\sigma_2^2}{25}+\sigma_1\right)\Bigg)\Bigg),\\
c_2&=\frac{c_1\left(\sigma_2^2b_1^2+\sigma_2\,b_1^2\sqrt{\sigma_2^2+40\,\sigma_1}+10\,\sigma_1\,b_1^2-10\,\sigma_1\,c_1^2\right)}{2\sigma_2\,\sigma_1},\\
c_3&=\frac{5\,c_1}{36\,\sigma_1\,\sigma_2^2}\Bigg(\Bigg(\left(\frac{1}{10}\,\sigma_2{}^3\sqrt{\sigma_2^2+40\,\sigma_1}+\frac{1}{10}\,\sigma_2{}^4\right.\\
&\left.+\sigma_2\sqrt{\sigma_2^2+40\,\sigma_1}\sigma_1+3\,\sigma_1\,\sigma_2^2+5\,\sigma_1{}^2\right)b_1^4-\left(\frac{2}{5}\,\sigma_2^2+\sigma_1\right)b_1^2\\
&\left(\sqrt{\sigma_2^2+40\,\sigma_1}\sigma_2+\sigma_2^2+10\,\sigma_1\right)c_1^2+5\,\sigma_1\,c_1^4\left(\frac{4\,\sigma_2^2}{25}+\sigma_1\right)\Bigg)\Bigg),\eta_0=0,\\
&\eta_1=0\quad\&\quad b_0,b_1,c_0,c_1,\eta_2,\eta_3=\text{free parameters}.
\end{aligned}\tag{32}$$

Taking these values into account along with (31), then using (4), we obtain the solution of (1).

Note 1: It is worthy to be noted that the correctness of all solutions has been checked by placing them in the main equation. Further, the entire achieved solutions are new and have not been presented in previous research.

Note 2: It is necessary to use symbolic software such as Mathematica or Maple to handle the required calculations in this paper.

Conclusion

Finding analytical solutions to many partial differential equations is very hard or even impossible in many cases. Therefore, the study of existing methods that are able to find analytical solutions to such equations is of great importance. Moreover, the performance of such techniques should always be revisited to increase their effectiveness as much as possible. This fundamental point necessitates that researchers always move in the direction of improving performance as well as discovering new methods in determining the analytical solutions of such equations. In this contribution, a reliable method for obtaining analytical solutions of the generalized Caudrey–Dodd–Gibbon–Kotera–Sawada equation based on Hirota's bilinear form idea is utilized. The forms obtained for equation solutions in this paper are different categories, including the collision of lump wave and a strip soliton, lump

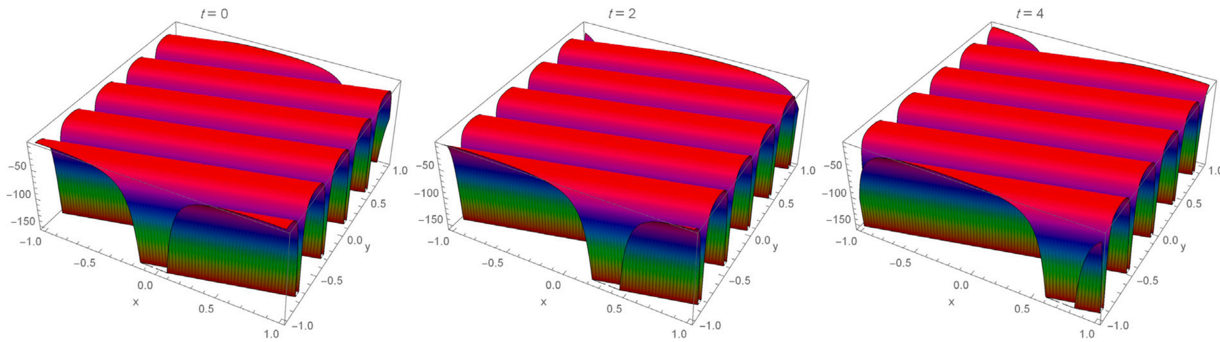

Fig. 6. Numerical simulations corresponding to Eq. (30).

wave and a double stripes soliton, lump and periodic waves, and finally lump wave and a double stripes soliton. The novel structures proposed in this paper may lead to the introduction of new applications for the generalized Caudrey–Dodd–Gibbon–Kotera–Sawada equation in some real-world problems. Further, several 3D diagrams of some of the resulting solutions have been included in the article. The main methodology used in this paper and its corresponding solutions introduced are of great importance because they may be effective in interpreting some physical phenomena in different fields of applied mathematics.

Declaration of competing interest

The authors declare that they have no known competing financial interests or personal relationships that could have appeared to influence the work reported in this paper.

Funding

This research work is not supported by any funding agencies.

References

[1] Atangana A. Exact solution of the time-fractional groundwater flow equation within a leaky aquifer equation. J Vib Control 2016;22(7):1749–56.
[2] Yel G, Cattani C, Baskonus HM, Gao W. On the complex simulations with dark–bright to the hirota–maccari system. J Comput Nonlinear Dyn 2021;16(6):061005.
[3] Duffy DJ. Finite difference methods in financial engineering: A partial differential equation approach. John Wiley & Sons; 2013.
[4] Ikram MD, Asjad MI, Akgül A, Baleanu D. Effects of hybrid nanofluid on novel fractional model of heat transfer flow between two parallel plates. Alexandria Eng J 2021;60(4):3593–604.
[5] Ma WX, Zhang Y, Tang Y, Tu J. Hirota bilinear equations with linear subspaces of solutions. Appl Math Comput 2012;218(13):7174–83.
[6] Pashaev O, Tanoğlu G. Vector shock soliton and the hirota bilinear method. Chaos Solitons Fractals 2005;26(1):95–105.
[7] Inc M, Miah M, Akher Chowdhury SA, Rezazadeh H, Akinlar MA, Chu YM. New exact solutions for the kaup-kupershmidt equation. AIMS Math 2020;5(6):6726–38.
[8] Glowinski R, Neittaanmäki P. Partial differential equations: Modelling and numerical simulation, Vol. 16. Springer Science & Business Media; 2008.
[9] Gao W, Veeresha P, Prakasha DG, Baskonus HM, Yel G. New numerical results for the time-fractional phi-four equation using a novel analytical approach. Symmetry 2020;12(3):478.
[10] Fischer B, Modersitzki J. Fast inversion of matrices arising in image processing. Numer Algorithms 1999;22(1):1–11.
[11] Inc M, Rezazadeh H, Vahidi J, Eslami M, Akinlar MA, Ali MN, Chu YM. New solitary wave solutions for the conformable klein-gordon equation with quantic nonlinearity. AIMS Math 2020;5(6):6972–84.
[12] Gao W, Veeresha P, Prakasha DG, Baskonus HM. New numerical simulation for fractional benney–lin equation arising in falling film problems using two novel techniques. Numer Methods Partial Differential Equations 2021;37(1):210–43.
[13] Ghalib MM, Zafar AA, Farman M, Akgül A, Ahmad M, Ahmad A. Unsteady mhd flow of maxwell fluid with caputo–fabrizio non-integer derivative model having slip/non-slip fluid flow and newtonian heating at the boundary. Indian J Phys 2021;1–10.
[14] Ma WX. Lump solutions to the kadomtsev–petviashvili equation. Phys Lett A 2015;379(36):1975–8.
[15] Yépez-Martínez H, Gómez-Aguilar J, Atangana A. First integral method for non-linear differential equations with conformable derivative. Math Model Nat Phenom 2018;13(1):14.
[16] Wang H. Lump and interaction solutions to the (2+ 1)-dimensional burgers equation. Appl Math Lett 2018;85:27–34.
[17] Leta TD, Liu W, El Achab A, Rezazadeh H, Bekir A. Dynamical behavior of traveling wave solutions for a (2+ 1)-dimensional bogoyavlenskii coupled system. Qual Theory Dyn Syst 2021;20(1):1–22.
[18] Hosseini K, Sadri K, Mirzazadeh M, Ahmadian A, Chu YM, Salahshour S. Reliable methods to look for analytical and numerical solutions of a nonlinear differential equation arising in heat transfer with the conformable derivative. Math Methods Appl Sci 2021. http://dx.doi.org/10.1002/mma.7582.
[19] Akgül A, Danish GA, Imran M, Waqas H, Tahir M, Asjad MI, Baleanu D. Effects of non-linear thermal radiation and chemical reaction on time dependent flow of williamson nano fluid with combine electrical mhd and activation energy. J Appl Comput Mech 2020.
[20] Wang C. Lump solution and integrability for the associated hirota bilinear equation. Nonlinear Dynam 2017;87(4):2635–42.
[21] Bielecki TR, Jeanblanc* M, Rutkowski M. Pde approach to valuation and hedging of credit derivatives. Quant Finance 2005;5(3):257–70.
[22] Khater MM, Ghanbari B, Nisar KS, Kumar D. Novel exact solutions of the fractional bogoyavlensky–konopelchenko equation involving the atangana-baleanu-riemann derivative. Alexandria Eng J 2020;59(5):2957–67.
[23] Atangana A, Kılıçman A. Analytical solutions of boundary values problem of 2d and 3d Poisson and biharmonic equations by homotopy decomposition method. Abstr Appl Anal 2013;2013.
[24] Ghanbari B, Günerhan H, Srivastava H. An application of the atangana-baleanu fractional derivative in mathematical biology: A three-species predator–prey model. Chaos Solitons Fractals 2020;138:109910.
[25] Gao W, Baskonus HM, Shi L. New investigation of bats-hosts-reservoir-people coronavirus model and application to 2019-ncov system. Adv Difference Equ 2020;2020(1):1–11.
[26] Wang C. Spatiotemporal deformation of lump solution to (2+ 1)-dimensional kdv equation. Nonlinear Dynam 2016;84(2):697–702.
[27] Hosseini K, Sadri K, Mirzazadeh M, Salahshour S. An integrable (2+ 1)-dimensional nonlinear schrödinger system and its optical soliton solutions. Optik 2021;229:166247.
[28] Rezazadeh H, Younis M, Eslami M, Bilal M, Younas U, et al. New exact traveling wave solutions to the (2+ 1)-dimensional chiral nonlinear schrödinger equation. Math Model Nat Phenom 2021;16:38.
[29] Ghanbari B, Raza N. An analytical method for soliton solutions of perturbed schrödinger's equation with quadratic-cubic nonlinearity. Modern Phys Lett B 2019;33(03):1950018.
[30] Meng F, Pang A, Dong X, Han C, Sha X. H∞ optimal performance design of an unstable plant under bode integral constraint. Complexity 2018;2018:1–10.
[31] Sheng H, Wang S, Zhang Y, Yu D, Cheng X, Lyu W, Xiong Z. Near-online tracking with co-occurrence constraints in blockchain-based edge computing. IEEE Internet of Things Journal 2020;8(4):2193–207.
[32] Xiao G, Song K, He Y, Wang W, Zhang Y, Dai W. Prediction and experimental research of abrasive belt grinding residual stress for titanium alloy based on analytical method. Int. J. Adv. Manuf. Technol. 2021;115:1111–25.
[33] Chen L, Xu J, Zhang M, Rong T, Jiang Z, Li P. Systematic study on mechanical and electronic properties of ternary VAlN, TiAlN and WAlN systems by first-principles calculations. Ceram. Int. 2021;47(6):7511–20.
[34] Fan P, Deng R, Qiu J, Zhao Z, Wu S. Well logging curve reconstruction based on kernel ridge regression. Arabian J. Geosci. 2021;14:1559.
[35] Li T, Dai Z, Yu M, Zhang W. Numerical investigation on the aerodynamic resistances of double-unit trains with different gap lengths. Eng. Appl. Comput. Fluid Mech. 2021;15(1):549–60.

[36] Li HW, Gao YF, Du CH, Hong WP. Numerical study on swirl cooling flow, heat transfer and stress characteristics based on fluid-structure coupling method under different swirl chamber heights and reynolds numbers. Int. J. Heat Mass Transfer 2021;73:121228.
[37] Ye R, Liu P, Shi K, Yan B. State damping control: A novel simple method of rotor UAV with high performance. IEEE Access 2020;8:214346–57.
[38] Zhang C, Kordestani H, Masri SF, Wang J, Sun L. Data-driven system parameter change detection for a chain-like uncertainties embedded structure. Struct. Control Health Monit. 2021;e2821.
[39] Chen X, Wang T, Ying R, Cao Z. A fault diagnosis method considering meteorological factors for transmission networks based on p systems. Eng. Appl. Comput. Fluid Mech. 2021;23(8):1008.
[40] Wang T, Liu W, Zhao J, Guo X, Terzija V. A rough set-based bio-inspired fault diagnosis method for electrical substations. Int. J. Electr. Power Energy Syst. 2020;119:105961.
[41] Wang T, Wei X, Wang J, Huang T, Peng H, Song X, Cabrera LV, Perez-Jimenez MJ. A weighted corrective fuzzy reasoning spiking neural P system for fault diagnosis in power systems with variable topologies. Eng. Appl. Artif. Intell. 2020;92:103680.
[42] Huang Z, Wang T, Liu W, Valencia-Cabrera L, Pe'rez-Jime'nez MJ, Li P. A fault analysis method for three-phase induction motors based on spiking neural p systems. Complexity 2021;2021:2087027.
[43] Luo J, Li M, Liu X, Tian W, Zhong S, Shi K. Stabilization analysis for fuzzy systems with a switched sampled-data control. J. Franklin Inst. 2020;375(1):39–58.
[44] Xie W, Zhang R, Zeng D, Shi K, Zhong S. Influence of mach number of main flow on film cooling characteristics under supersonic condition. Int. J. Robust Nonlinear Control 2020;30(5):1956–78.
[45] Zhang B, Chen YX, Wang ZG, Li JQ, Ji HH. Influence of mach number of main flow on film cooling characteristics under supersonic condition. Symmetry 2021;13(1):127.
[46] Hirota R. The direct method in soliton theory. Cambridge: cambridge univ. Pr; 2004.
[47] Rui W, Zhang Y. Soliton and lump-soliton solutions in the grammian form for the bogoyavlenskii–kadomtsev–petviashvili equation. Adv Difference Equ 2020;2020(1):1–12.
[48] Li L, Duan C, Yu F. An improved hirota bilinear method and new application for a nonlocal integrable complex modified korteweg-de vries (mkdv) equation. Phys Lett A 2019;383(14):1578–82.
[49] Wang C. Lump solution and integrability for the associated hirota bilinear equation. Nonlinear Dynam 2017;87(4):2635–42.
[50] Ma WX, Fan E. Linear superposition principle applying to hirota bilinear equations. Comput Math Appl 2011;61(4):950–9.
[51] Gao LN, Zhao XY, Zi YY, Yu J, Lü X. Resonant behavior of multiple wave solutions to a hirota bilinear equation. Comput Math Appl 2016;72(5):1225–9.
[52] Wazwaz AM. Multiple-soliton solutions for the kp equation by hirota's bilinear method and by the tanh–coth method. Appl Math Comput 2007;190(1):633–40.
[53] Ullah MS, Ali MZ, Roshid HO, Hoque MF. Collision phenomena among lump, periodic and stripe soliton solutions to a (2+1)-dimensional benjamin–bona–mahony–burgers model. Eur Phys J Plus 2021;136(4):1–9.
[54] Dong MJ, Tian SF, Yan XW, Zou L. Solitary waves, homoclinic breather waves and rogue waves of the (3+ 1)-dimensional hirota bilinear equation. Comput Math Appl 2018;75(3):957–64.
[55] Ghanbari B, Asadi E. New solitary wave solutions of the sawada-kotera equation and its bidirectional form. Phys Scr 2021.
[56] Deng GF, Gao YT, Su JJ, Ding CC, Jia TT. Solitons and periodic waves for the (2+ 1)-dimensional generalized caudrey–dodd–gibbon–kotera–sawada equation in fluid mechanics. Nonlinear Dynam 2020;99(2):1039–52.
[57] Konopelchenko B, Dubrovsky V. Some new integrable nonlinear evolution equations in 2+ 1 dimensions. Phys Lett A 1984;102(1–2):15–7.
[58] Sawada K, Kotera T. A method for finding n-soliton solutions of the kdv equation and kdv-like equation. Progr Theoret Phys 1974;51(5):1355–67.
[59] Peng WQ, Tian SF, Zou L, Zhang TT. Characteristics of the solitary waves and lump waves with interaction phenomena in a (2+ 1)-dimensional generalized caudrey–dodd–gibbon–kotera–sawada equation. Nonlinear Dynam 2018;93(4):1841–51.
[60] Hu XB, Li Y. Some results on the caudrey-dodd-gibbon-kotera-sawada equation. J Phys A: Math Gen 1991;24(14):3205.
[61] Lou Sy. Twelve sets of symmetries of the caudrey-dodd-gibbon-sawada-kotera equation. Phys Lett A 1993;175(1):23–6.
[62] Chan W, Zheng Yk. Bäcklund transformations for the caudrey–dodd–gibbon–sawada–kotera equation and its λ-modified equation. J Math Phys 1989;30(9):2065–8.
[63] Saha Ray S. New soliton solutions of conformable time fractional caudrey–dodd–gibbon–sawada–kotera equation in modeling wave phenomena. Modern Phys Lett B 2019;33(18):1950202.
[64] Baleanu D, Inc M, Yusuf A, Aliyu AI. Lie symmetry analysis, exact solutions and conservation laws for the time fractional caudrey–dodd–gibbon–sawada–kotera equation. Commun Nonlinear Sci Numer Simul 2018;59:222–34.
[65] Kumar D, Kumar S. Some more solutions of caudrey–dodd–gibbon equation using optimal system of lie symmetries. Int J Appl Comput Math 2020;6(4):1–11.
[66] Hirota R. Exact solution of the korteweg—de vries equation for multiple collisions of solitons. Phys Rev Lett 1971;27(18):1192.
[67] Lü X, Chen SJ. Interaction solutions to nonlinear partial differential equations via hirota bilinear forms: One-lump-multi-stripe and one-lump-multi-soliton types. Nonlinear Dynam 2021;103(1):947–77.
[68] Lu J, Duan X, Hong X, et al. Explicit solutions for the coupled nonlinear drinfeld–sokolov–satsuma–hirota system. Results Phys 2021;24:104128.
[69] Kumar S, Nisar KS, Kumar A. A (2+ 1)-dimensional generalized hirota–satsuma–ito equations: Lie symmetry analysis, invariant solutions and dynamics of soliton solutions. Results Phys 2021;104621.
[70] Cui P. Bilinear form and exact solutions for a new extended (2+ 1)-dimensional boussinesq equation. Results Phys 2021;22:103919.
[71] Aliyu AI, Li Y. Bell polynomials and lump-type solutions to the hirota–satsuma–ito equation under general and positive quadratic polynomial functions. Eur Phys J Plus 2020;135(1):1–10.